Calculation of Diesel Combustion in Idealised Chambers

R.J.R.Johns

Ricardo Consulting Engineers
Bridge Works, Shoreham-by-Sea, West Sussex, BN43 5FG
UK

ABSTRACT

The paper describes results from the further development of a detailed model for diesel combustion. Specifically, this study focuses on the sensitivity of computed ignition delay to various physical and numerical parameters, including initial drop size, mixing rate and mesh density. The behaviour observed is explained in terms of different processes and how they are reflected in the modelled equation system. Finally, results from a typical three-dimensional calculation are described.

INTRODUCTION

One of the main reasons for developing detailed mathematical models of diesel combustion is to gain a better understanding of the processes involved and to have a tool that is of benefit for the development of practical combustion systems. Unfortunately, many of the individual phenomena involved, such as atomization, turbulent mixing and chemistry, are either too complicated or are insufficiently understood to allow modelling that is representative under all conditions. As a result, models often contain numerous 'tunable' coefficients that may or may not be related to some identifiable quantity but which detract from the overall generality if they cannot be assigned appropriate values in a meaningful way. To avoid this, modellers often adopt a pragmatic approach whereby simplified representations and mechanisms are introduced in order to progress whilst experimental data, cast in appropriate mathematical form, fills in remaining gaps. Most modellers use a "bottom up" approach whereby each stage in the model development is checked, usually by reference to experimental data, before proceeding to the next.

Whilst there have been some outstanding successes, there are also areas where substantially different models give similar results: the modelling of spray dynamics in reciprocating engines is a good example. In this case, it would appear that certain characteristics of sprays, for example, the penetration of non-evaporating sprays, are relatively insensitive to the precise details of initial conditions and modelling. This is unfortunate because conclusions about a model's correctness based on the reproduction of experimental data at low temperature are not necessarily valid at high temperature.

There is a further complication, namely that of eliminating effects resulting from errors in the numerical solution. The usual sources of such errors, namely grid and time step dependence, flow orientation to the mesh and, for Monte-Carlo solution methods, statistical errors arising from low sampling rates, are all apparent in spray calculations and have been demonstrated to have a significant effect on the results. The purpose of this paper is to clarify some of these problems in a systematic way and to demonstrate results from a model of diesel combustion.

CONTENTS OF PAPER

The work reported in this paper is based upon the simplified Probability Density Function (pdf) model of diesel combustion described in (1). The key features of the model and previous efforts at correlating with experimental data are briefly described. During the course of model development, it was found that calculations were sensitive to some important parameters of the model and aspects of the numerical technique. In particular, droplet size and mesh density have been found to be sensitive parameters and a detailed study is described of their effect on computed ignition delay. Clearly, in a model in which empiricism is inevitable, for example, in the modelling of ignition chemistry, it is vital either to eliminate or quantify as many uncertainties as possible.

Unlike many other models of diesel combustion, the simplified PDF model explicitly allows for mixing between fuel, oxidant and combustion products such that different mixed states may coexist at a particular time and location. Whilst this approach allows a greater level of generality, it also introduces an additional degree of freedom in that the ignition delay and "premixed" burning are dependent upon the rate of mixing. Results are presented which demonstrate the influence of the mixing rate on computed ignition delay.

Finally, results of a 3-dimensional combustion calculation are described. This is typical of test

calculations currently being performed to try and clarify the behaviour of the model under realistic injection and swirl conditions. Results are presented in terms of the temperature and velocity fields at different times and the heat release rate.

DESCRIPTION OF THE MODEL

The model has been extensively described in a previous paper (1) and therefore only a brief description and any significant differences between current and previous practice are given here.

The model consists of three inter-related parts, namely: calculation of the gas phase velocity, pressure and turbulence; the combustion model; and modelling of spray dynamics. The first of these employs standard equations for the conservation of momentum and mass, with the effects of turbulence represented using the k-ε model.

Combustion is modelled by assuming that the probability density function of composition space can be represented by Dirac delta functions of fuel, oxidant and combustion products and their associated mixed states. Thus, a continuous distribution of composition and temperature is reduced to seven distinct states which vary with both space and time, namely (i) Fuel, (ii) Oxidant, (iii) Products, (iv) Fuel + Oxidant, (v) Oxidant + Products, (vi) Products + Fuel and (vii) Fuel + Oxidant + Products. Figure 1 shows schematically composition space and the different states. The different states are referred to as 'elements' and the dependent variables are the density-weighted ensemble-averaged probabilities of each; these can also be thought of as the mass fractions of each element. In addition to the differences in composition between the elements, each has its own temperature.

Various physical processes affect the distribution, including: transport in physical space (convective and turbulent, the latter modelled as a diffusion process); turbulent mixing (modelled using Curl's binary mixing model (2)), which changes the distribution but not the mean composition; reaction (the 'Shell knock model' (3) as modified by Theobald (4) is used for auto-ignition, whilst the main combustion is modelled with either a 2-step kinetics scheme or a simpler 'mixed-is-burned' assumption applied to element (vii)); and fuel source generation (renormalization).

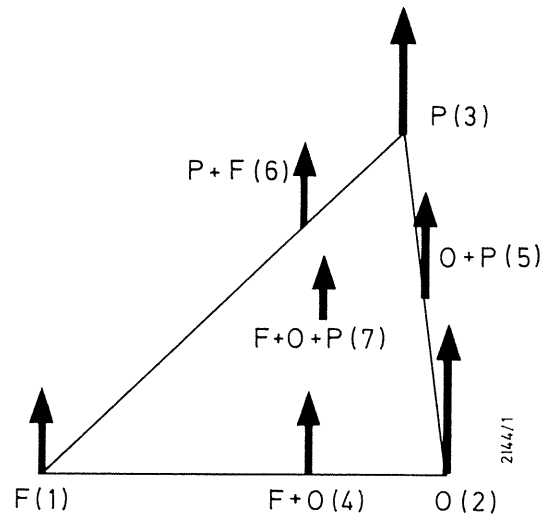

Figure 1 - Representation of simplified PDF
F = Fuel, O = Oxidant, P = Products

Modelling of the spray dynamics is based on the Discrete Droplet Model originally described in (5). However, during the past few years, a number of different practices have evolved for determining the initial droplet size distribution and the various physical processes that subsequently determine the downstream size; these can be categorised as follows:

1) Gosman and Johns (5) introduced droplets based upon a typical distribution measured downstream.
2) O'Rourke (6) used a modified form of Taylor's (7) and Ranz's (8) aerodynamic breakup theory to specify both the initial drop size and spray angle. A model for droplet collisions was developed which provided a mechanism for downstream growth in drop size.
3) O'Rourke and Amsden (9) and Reitz and Diwaker (10) proposed that droplets could be introduced equal to the nozzle hole diameter and that a model for droplet breakup would produce smaller droplets resulting from atomization. As with method 2), coalescence provides the mechanism for downstream growth.

Not surprisingly, the three methods give different behaviour for the variation of drop size along the spray axis for the relatively simple case of a non-evaporating spray: method 1 gives a value unchanged from that at the injector; method 2 gives a monotonic growth whilst method 3 gives an initially large drop size, followed by a rapid reduction and then increase. It is interesting that all three approaches are capable of yielding reasonable agreement with experimental spray tip penetration data, spray angle and downstream drop size.

However, the behaviour of these models under high pressure and temperature conditions and at injection rates typical of current high pressure injection systems produces difficulties. The main problem stems from the use of aerodynamic breakup models that produce very small (sub-micron) size droplets. The small droplets are strongly coupled to the gas phase and this results in a rapid exchange of momentum and energy and high evaporation rates. The strong coupling may also lead to numerical difficulties in resolving steep gradients near the spray axis and close to the injector. It has been observed by both the present author and others (11) that the combination of small drop sizes and inadequate mesh resolution produces sprays that have low axial penetration, excessive radial dispersion, higher evaporation rates and, where an ignition sub-model is used, too short ignition delays.

In this study, it is accepted that the phenomenon of atomisation is not yet properly understood and to remove uncertainties associated with small drops described above, models of droplet breakup and coalescence have not been used. Instead, correlations of initial spray angle and drop size, the latter based on experimental data measured some distance downstream of the injector, have been employed.

Spray Angle

Spray angle is based on the aerodynamic breakup theory, modified by Reitz (12) to account for variations in nozzle l/d ratio. This correlation is given by:

$$\frac{\theta}{2} = \tan^{-1}\left\{\frac{4\pi}{3 + 0.28\,\ell/d}\sqrt{\frac{\rho_g}{\rho_\ell}}\; f\left(\frac{\rho_\ell}{\rho_g}\left(\frac{Re_\ell}{We_\ell}\right)^2\right)\right\} \quad (1)$$

where f is a function fitted to data in ref. (12).

Equation 1 has been found to give reasonable correlation between the measured and computed spray angle for high pressure and ambient temperature conditions. Figure 2 shows the level of agreement for a variety of different injection systems, further details of which are given in Table 1.

Initial Drop Size

The correlation used here is based on the work of Elkotb (16). Although the experimental work from which the correlation is derived is for a pintle nozzle, there is good evidence that breakup mechanisms and the resulting downstream drop size for hole nozzles is similar (13). The relationship is given by:

$$\bar{d}_{32} = 3.08\left(\frac{\mu_\ell}{\rho_\ell}\right)^{0.385}(\sigma\rho_\ell)^{0.737}\,\rho_g^{0.06}\left\{\left(\frac{V_{inj}}{C_{dis}}\right)^2\frac{\rho_\ell}{2}\right\}^{-0.54} \quad (2)$$

where the symbols have their usual meanings. A comparison between measured and calculated downstream drop sizes for two different injection systems (refs. (13,14)) is shown in figure 3. Whilst it might be argued that this approach includes neither coalescence nor breakup effects, it is reasonably reliable in determining downstream drop size and does not produce spurious ignition delays resulting from sub-micron droplets.

TEST GEOMETRY AND CONDITIONS

The combustion bomb experiments of ref. (17) have been used as a reference set of data for the parameter studies described in this paper. The same data have been used previously by Theobald (4) and Johns (1) for the development and testing of diesel combustion models. These data span the gas pressure and temperature range $11 < P_{gas} < 31$ (bar) and $670 < T_{gas} < 880$ (K). Various other details relating to the computations are given below:

- Computational domain: 100mm (axial) x 30mm (radial)
- Mesh:all calculations have used a 2D (axisymmetric) mesh with uniform spacing in both directions. Examination of the effects of mesh dependency has used the following mesh sizes:

0.5mm	(axial)	x	0.375mm	(radial)	- MESH1
1.0mm	"	x	0.75mm	"	- MESH2
2.0mm	"	x	1.50mm	"	- MESH3

- Unless stated otherwise, all calculations have been repeated 3 times with different random number seeds (used, among other things, for sampling the spray initial conditions). The droplet parcel introduction rate was 800 /ms for all calculations.

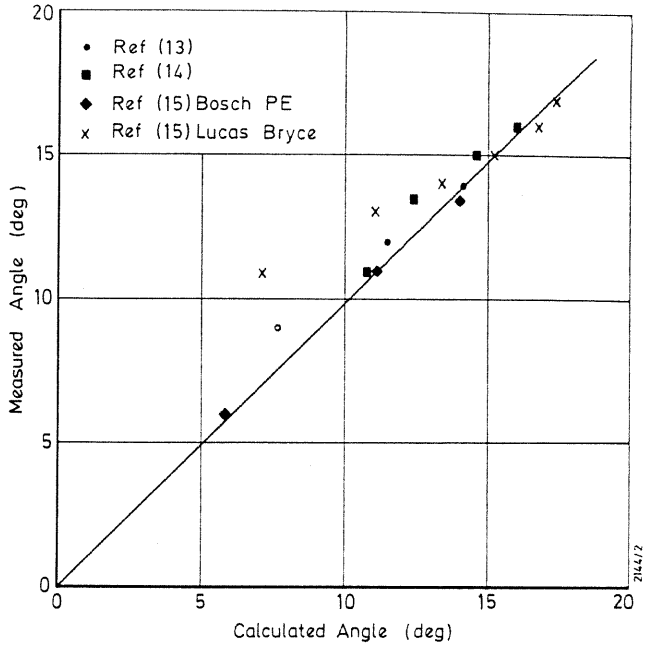

Figure 2 - Comparison between measured and computed spray angles (Equation 1)

TABLE 1.
INJECTION SYSTEM AND EXPERIMENTAL CONDITIONS FOR SPRAY ANGLE COMPARISON

Ref.	Injection System	Nozzle l/d ratio	Nozzle d (mm)	Bomb Pressure Range (bar)
13	Bosch PE	6.7	0.3	1 - 50
14	?	3.7	0.29	26 - 81
15	Bosch PE	3.6	0.213	5 - 45
15	Lucas Bryce	1.65	0.46	5 - 50

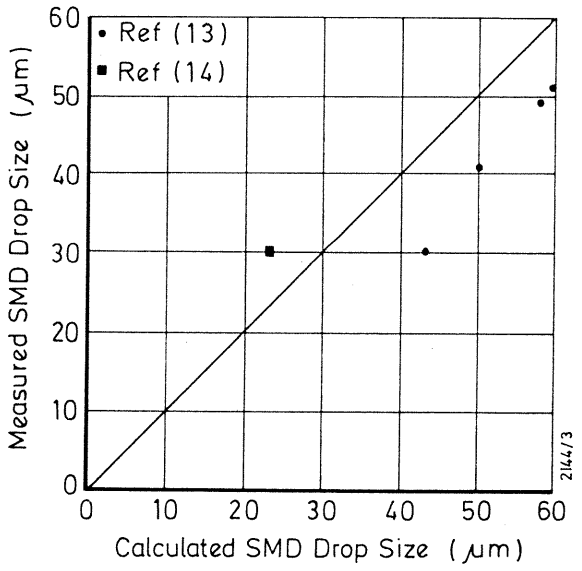

Figure 3 - Comparison between measured and computed drop sizes (Equation 2)

The computational time step for the partial differential equations was 1μs, whilst the spray and chemistry models used time steps determined by error estimators within their own solvers.

- Ignition was assumed to have occurred if the rate of change of temperature was greater than 10^7 degrees/s or the temperature in a cell exceeded 1200 K.

COMPARISON WITH EXPERIMENTAL IGNITION DELAY

Using the Elkotb (16) correlation produces initial droplet sizes considerably greater than those used by either Theobald (4) or Johns (1) in previous studies on ignition delay. For example, at the highest bomb pressure (31 bar) and temperature (880 K), equation 2 gives a Sauter mean diameter of 43μm compared with a value of 3μm from aerodynamic theory. Theobald obtained reasonable agreement with experimental ignition delays by modifying one of the coefficients in the original Shell model. However, drop size has a considerable influence on computed delay, as discussed below, and it was found that the increased initial drop size (43μm vs 3μm) doubled the duration of the ignition delay. To compensate for this, the coefficient Af4 in the Shell model was assigned a value 4x that used in previous work (4,1). The comparison with experimental data is shown in figure 4 (note: only the higher pressures and temperatures have been used for this exercise and the bomb length was extended to 150mm to avoid excessive impingement at the 750 K condition). The level of agreement with the larger initial drop size and increased coefficient is similar to that obtained originally. It is also clear that the temperature dependence is over-estimated, as in previous work, indicating that some more fundamental revisions are needed to the auto-ignition chemistry model, although this is not addressed here.

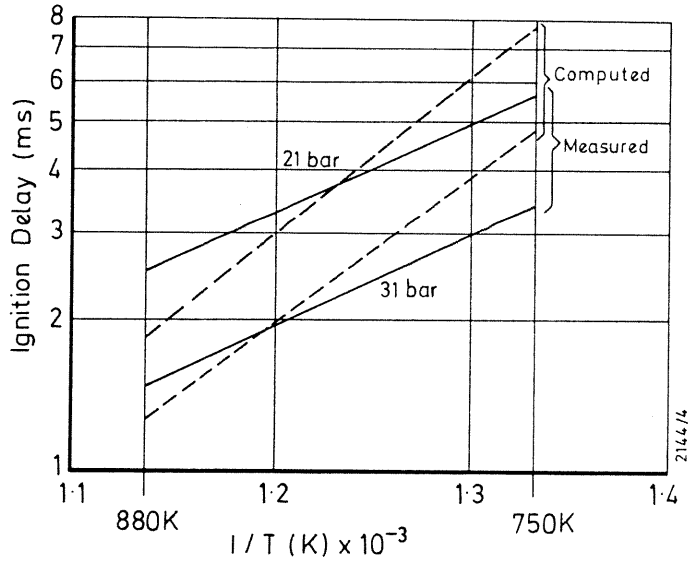

Figure 4 - Comparison between measured and computed ignition delays

EFFECT OF INITIAL DROP SIZE

The highest pressure and temperature condition (31 bar and 880 K) has been used for the study described below of initial drop size, grid dependence and mixing rate.

Figure 5 shows the effect of initial drop size on computed ignition delay. The initial sizes span the range 1 - 40μm. The individual points indicate the separate runs that have been averaged to give the mean data for the MESH2 mesh. It can be seen that there is little scatter between the runs for each condition but more than a factor of 2 between the limiting values of drop size. Figure 6 shows the corresponding total mass of fuel evaporated during the delay period for initial drop sizes of 1, 10 and 40μm.

EFFECT OF MESH SIZE

The mesh size was varied in both axial and radial

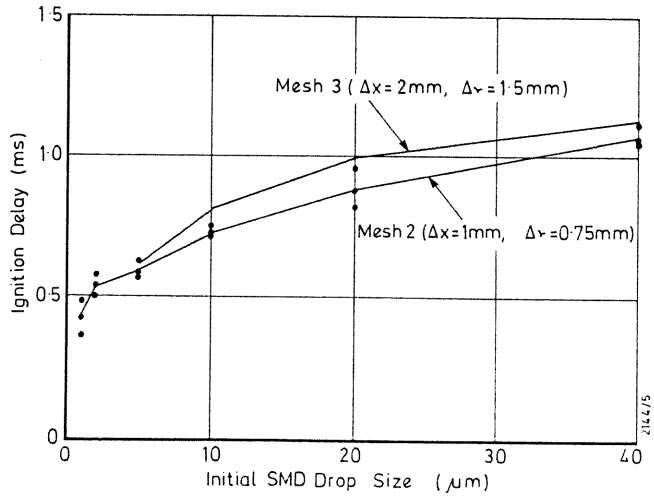

Figure 5 - Effect of initial drop size and mesh density on computed ignition delay

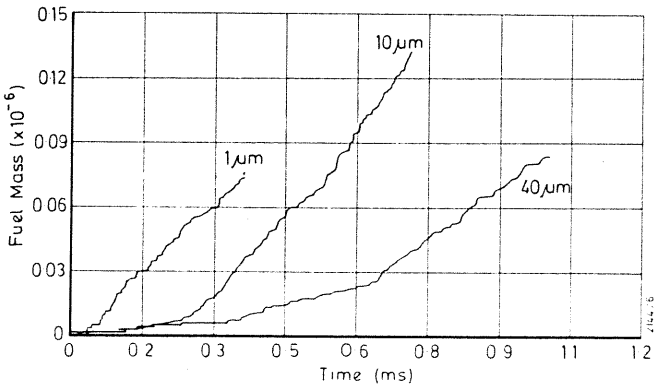

Figure 6 - Effect of initial drop size on fuel evaporated

directions as described above. Results of the run-averaged ignition delay for the coarsest mesh (MESH3) are shown in figure 5. Here, there is a clear indication of increasing ignition delay with the higher mesh spacing. The finer mesh (MESH1) results have not been plotted as they were practically indistinguishable from the MESH2 data, with the exception of the 1 and 2μm drop sizes. It is concluded that, for the particular conditions of this simulation, the MESH2 results are grid independent.

At the smallest droplet sizes with the finest mesh, a phenomenon was observed whereby ignition could occur after just a few time steps. Although this is still under investigation, it would appear that the following mechanism is responsible. Fluctuations in gas phase properties (temperature, density etc.) occur because of the intermittent interaction of individual droplet parcels with any particular cell. This is a direct consequence of using a Monte Carlo method and is unavoidable. The level of fluctuation depends upon the amount of interaction between the droplet parcel and the cell and the frequency that different droplet parcels interact with the cell. The factors, therefore, that will tend to increase the level of fluctuation are:

1) small droplets (stronger gas-liquid coupling)
2) small cells (firstly, the time dependent term in the differential equations becomes smaller in relation to the source interaction term, thus the cell effectively has a lower 'inertia', and secondly, the frequency of interaction is reduced if the same number of droplet parcels must interact with an increased number of cells)
3) larger droplet parcels, resulting from a lower introduction rate (same reason as small cells).

The result of this is that fuel vapour mass fraction and temperature excursions that result from the Monte-Carlo method used for the spray are sufficiently great to allow spurious ignition. The general lesson that can be learned from this exercise is that mesh density and droplet parcel introduction rate should be directly related to minimise the level of gas property fluctuation and consequences therefrom. No attempt has yet been made to quantify this relationship.

EFFECT OF MIXING RATE

The PDF model differs from many other models of diesel combustion in the respect that the state of mixedness of fuel, oxidant and combustion products is represented explicitly. Thus, at any location within the combustion chamber at a given time, the gas phase is characterised by 7 different states of composition and temperature, instead of 1 (see figure 1). One of the main processes that affects the probability of the elements is turbulent mixing. Two limiting cases can be easily identified: firstly, 'zero mixing', in which case evaporated fuel and oxidant would be unable to mix and neither ignition nor the transition to main combustion would occur (this case is of no practical interest); and secondly, 'infinitely fast mixing', whereby the composition could be defined by a single state instead of 7. This second case is of interest, as other multidimensional models using a similar approach to model ignition chemistry implicitly assume that mixing is infinitely fast and segregation does not exist.

It is hoped that the rate of mixing will be linked to the turbulent time-scale and calculations currently underway are directed at determining the nature of such a correlation. However, to reduce the complexity of this investigation and avoid unpredictable variations in mixing rate (R_{mix}) due to, for example, grid dependence of the turbulence field, the calculations described above on droplet size and mesh density have been made with an effectively infinite rate of mixing ($R_{mix} = 10^6$).

Figure 7 shows the changes in computed ignition delay with a variation in mixing rate over the range $10^3 < R_{mix} < 10^6$. As with the droplet size investigations, 3 runs have been made at each condition and these are shown in the figure. There are a number of interesting

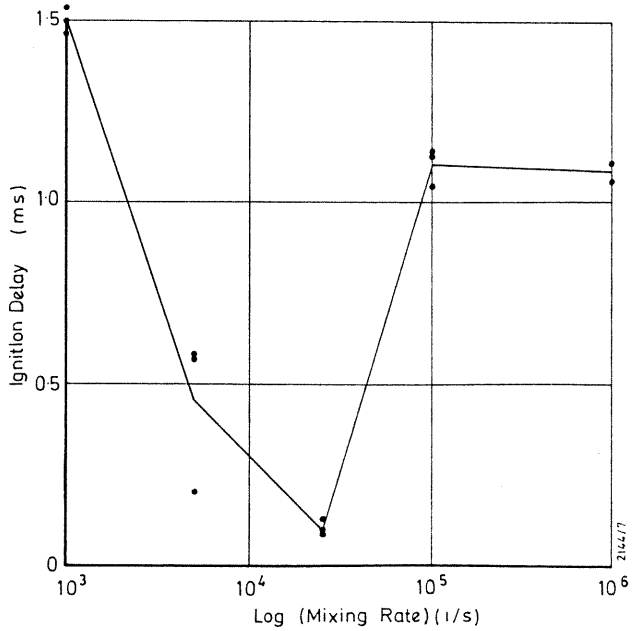

Figure 7 - Effect of mixing rate computed ignition delay

points to note from Figure 7: firstly, with the exception of the R_{mix}= $5x10^3$ 1/s data, there is very little scatter resulting from statistical variations, indicating a real trend; secondly, there are clearly two different regimes at high and low values and a minimum at an intermediate value of mixing rate.

Further examination of the mechanisms contributing to this behaviour have revealed the following. At high mixing rates before ignition occurs, the fuel and oxidant are effectively homogeneously mixed within a cell and the probability of the fuel+oxidant element is unity, indicating that all of the cell mass is contained in this element. At low mixing rates, the probability of the fuel+oxidant element is substantially less than unity whilst the separate fuel and oxidant elements contain most of the cell mass.

The mixing rate therefore has a considerable influence on the temperature and composition histories of the fuel+oxidant element - the element for which the auto-ignition reaction equations are solved. At high mixing rates, the temperature remains relatively high, as it is dominated by the cell gas temperature, whilst the fuel vapour mass fraction is low because the evaporated fuel is mixed with the entire cell contents. At low mixing rates, the situation is reversed with the fuel+oxidant element containing considerable fuel vapour but at a lower temperature, the latter because the mixed temperature is dominated by the temperature at which the vapour is evaporated from the droplet.

COMBUSTION

In the development of this diesel combustion model, the author has tried to balance fundamental studies, such as those described above, with computations at conditions more representative of current engines. The calculation described here is one of many that have been performed at more realistic conditions and includes a substantial part of the combustion period. The main computational details are given below:

- 3-dimensional, 72 degree sector of 20mm radius and 20mm depth. Mesh spacing: 0.8mm (radial) x 2mm (axial); Variable circumferential mesh spacing with 2 degrees at spray axis. Cyclic boundary conditions. Injection directed radially outwards with injector located at r = 5mm. Droplet parcel introduction rate = 800 /ms.
- P_{gas} = 31 bar; T_{gas} = 880 K; Initial swirl equivalent to Swirl Ratio = 4 @ 1000 rev/min.
- Nozzle diameter = 0.21 mm; nozzle l/d = 4.8; mass of fuel injected = 6.9 mg; injection period = 1.25 ms; computed Sauter mean diameter = 8μm; half spray angle = 4.8°

The mixing rate has been specified as $R_{mix} = 10^6$, giving an effectively infinite rate of mixing. The effects of dissociation have been included, somewhat crudely, by specifying $[CO]/[CO_2] = 0.3$. As heat release is associated with the CO oxidation step, this effectively reduces the lower calorific value of the fuel by 30%.

Figures 8 to 13 show the temperature and velocity fields from 0.06 ms to 2 ms. Ignition has already occurred by 0.06 ms, suggesting that either, at this stage of the calculation, conditions are appropriate for a minimum in the delay period, as discussed earlier, or the small mesh cell volume near the injector has resulted in spurious ignition. Interestingly, the velocity field surrounding the spray in figures 8 and 9 is different from it's non-combusting counterpart, showing a region of recirculating flow the entire length of the spray.

Figures 10 and 11 show that the spray quickly re-establishes after ignition. However, evaporation during combustion is sufficiently rapid that the quantity of liquid fuel in the system (not shown) is practically zero throughout the injection period. In this case, momentum and energy exchange and the generation of fuel vapour occur very close to the injector and the mechanisms generating the flow structure are more closely allied to those of a gas jet than a liquid spray. The effect of swirl can also be seen in figures 10 and 11 in the respect that there is considerably more dispersion on the downstream side of the swirl (clockwise direction) The high temperatures are found in the periphery of the spray, indicating that reaction is occurring in the zone separating the fuel on the inside of the spray and the air outside.

The combined effects of swirl and impingement produce the structures shown in figures 12 and 13. Figure 12 is at the end of injection and both the velocity and temperature fields show the residual structure of the jet and a large high temperature region. The latter has been generated by dispersion of the fuel vapour on the downwind side of the upstream spray and it is seen here due to the coupling introduced by the cyclic boundary condition. In figure 13, all residual traces of the spray structure have disappeared and, apart from a region close to the wall, the burning mixture occupies a single large volume in the combustion chamber and rotates with the swirl. There remain significant variations in temperature within the chamber well into the period of slow diffusion burning. The cooler region in the centre of the combustion zone is caused by the fuel vapour, this being unable to burn because of a lack of oxidant.

Figure 14 shows the integrated evaporated fuel and the amount of fuel vapour within the combustion chamber, the latter summed over all pdf elements. The difference between these at any instant of time represents the integral heat release. Although not plotted here, the mass of fuel injected is indistinguishable from the integrated evaporated fuel, as mentioned earlier. Also plotted on this graph, but remaining at a value of practically zero, is the integral over the field of the quantity: $\min\{M_{fu}, M_{ox}/S\}$, where M_{fu} and M_{ox} are respectively the masses of fuel and oxidant in a grid cell, S is the mass stoichiometric ratio and "min" is the minimum operator. Thus, this quantity will take a positive value whenever there is both fuel and oxidant in a cell (regardless of whether they are mixed or not). This is a strong indication that, for this particular case, combustion is a diffusion-controlled process throughout and the rate of heat release is determined by the rate at

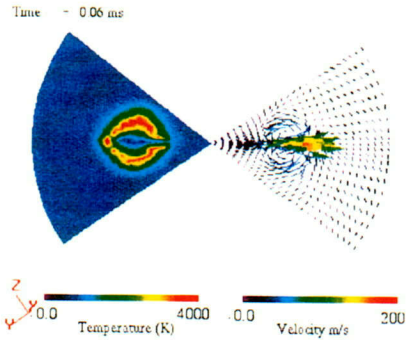

Figure 8

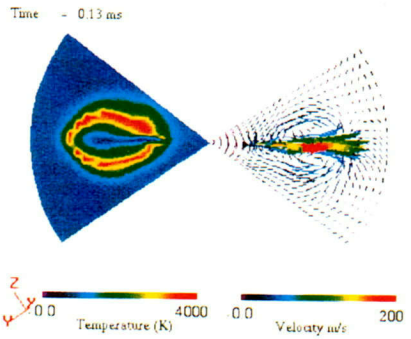

Figure 9

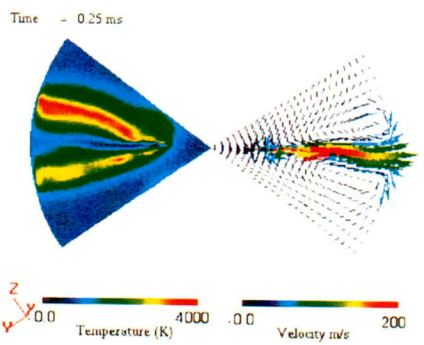

Figure 10

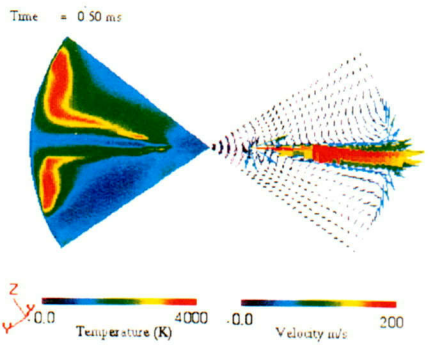

Figure 11

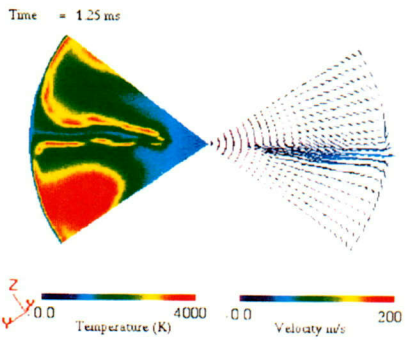

Figure 12

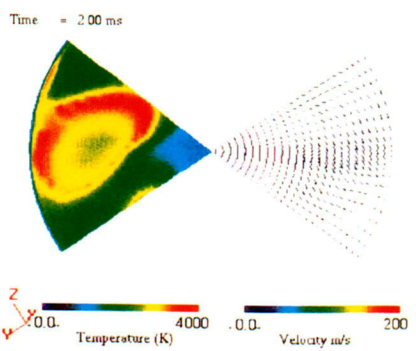

Figure 13

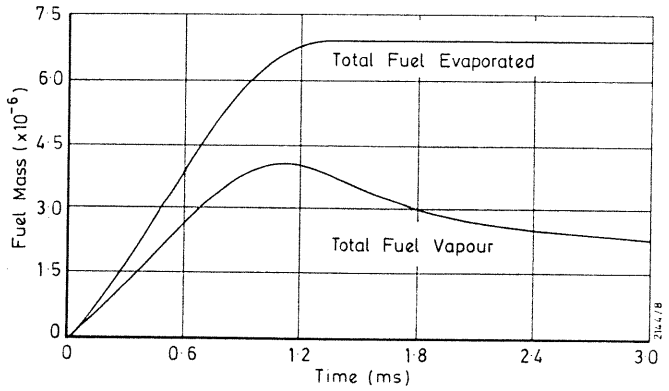

Figure 14 - Total fuel evaporated and amount of fuel vapour

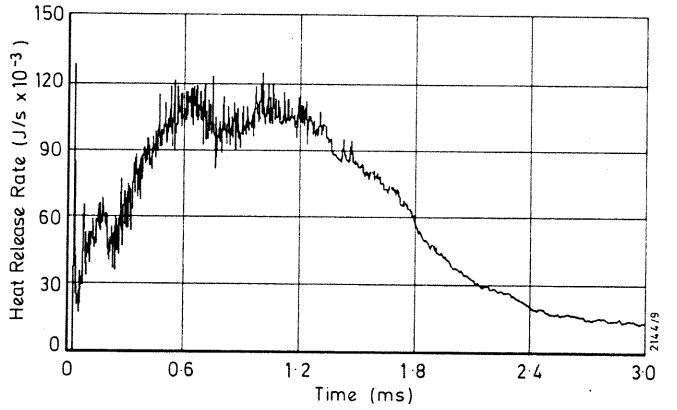

Figure 15 - Heat release rate

which fuel can diffuse away from the central core of the spray and air can diffuse inwards to the reaction zone.

The corresponding heat release rate is shown in figure 15. This shows a small but identifiable amount of pre-mixed burning because of the short ignition delay. The heat release rate up to approximately 1.5 ms appears to be controlled by two main factors: firstly, the surface area separating the zones containing fuel and oxidant and, secondly, the turbulent transport coefficient, the latter determined directly from the k- ε turbulence model. Both of these are significantly higher during this period due to the momentum and entrainment of the jet and wall impingement. After 2 ms the heat release rate is substantially reduced. The diffusion-controlled process is even clearer at this stage, with a single identifiable volume of hot combustion products containing a cooler core of fuel vapour and surrounded by the remaining air.

SUMMARY

The work described in this paper has examined the sensitivity of computed ignition delay to a number of parameters, both physical and numerical. The effects of initial drop size, mesh density and mixing rate have been quantified for a particular set of injection and bomb conditions. A practice has been adopted for specifying initial drop sizes and spray angle based on observations made in non-evaporating sprays. Whilst it is appreciated that this does not recognise mechanisms of breakup and coalescence, it does solve a major problem associated with the generation of sub-micron droplets produced by breakup models when used in conjunction with high pressure injection systems.

The results of the fundamental investigations can be summarised as follows:

1) Smaller initial drop sizes result in shorter ignition delays, with substantial reductions for sizes less than 5μm.
2) Coarser meshes produce longer ignition delays, although grid independent results were obtained using a mesh spacing of 1 mm axial x 0.75 mm radial, with only minor differences for a mesh 2x coarser.
3) Unpredictable behaviour may occur with very fine meshes and this appears to be due to the level of temperature and fuel vapour mass fraction variations resulting from statistical fluctuations.
4) The rate of mixing has an important influence on ignition delay. Two limiting regimes have been identified, depending on the temperature and fuel mass fraction. Further work is required to identify the mixing rate operating regimes of practical injection systems.
5) The current form of the ignition chemistry sub-model shows incorrect dependence on temperature and further work is necessary to improve the model at high pressures and temperatures.

The combustion model shows reasonable behaviour for the particular conditions of the calculation. Although the ignition delay was too short to produce any significant premixed burning, the mechanisms controlling the heat release rate were clearly identifiable with the flame structure. The instantaneous "flame area" and spatial turbulent transport, modelled as a diffusion process in the framework of the k-ε model, was the main rate-determining step. Thus, the rate of heat release for this case is independent of mixing rate.

Future effort will focus on refining those aspects of the model identified as requiring further work. These include the ignition chemistry sub-model, guidelines for the combined effects of droplet introduction rate and mesh size, and linking of the rate of mixing to the turbulence field.

REFERENCES

1) Johns, R.J.R. 'Progress in the development of a detailed model for diesel combustion', Int. Symp. COMODIA 90, 1990.

2) Curl, R.L., 'Dispersed phase mixing: 1. Theory and effects in simple reactors', A.I.Ch.E.J., Vol.9, pp 175-181, 1963.

3) Halstead, M.P., Kirsch, L.J. and Quinn, C.P., 'The autoignition of hydrocarbon fuels at high temperatures and pressures - fitting of a mathematical model', Combustion and Flame, Vol. 30, pp. 45-60, 1977.

4) Theobald, M.A., 'Numerical simulation of diesel autoignition', Ph.D. Thesis, MIT, 1986.

5) Gosman, A.D. and Johns, R.J.R., 'Computer analysis of fuel-air mixing in direct injection engines', SAE 800091, SAE Trans. 1980.

6) O'Rourke, P., 'Collective drop effects on vaporizing liquid sprays', Ph.D. Thesis, Princeton Univ., 1981.

7) Taylor,G.I., 'Generation of ripples by wind blowing over a viscous fluid', Collected works of G.I. Taylor, Vol. 3, 1940, p. 244.

8) Ranz, W.E., 'Some experiments on orifice sprays', Canad. J. Chem. Eng., Vol. 36, 1958, p.175.

9) O'Rourke, P.J. and Amsden, A.A, 'The tab method for numerical calculation of spray droplet breakup', SAE 872089.

10) Reitz, R.D. and Diwakar, R., 'Structure of high-pressure fuel sprays', SAE 870598.

11) Gonzalez, M.A., Lian, Z.W. and Reitz, R.D., 'Modeling diesel engine spray vaporization and combustion', SAE 920579.

12) Reitz, R.D., 'Atomization and other breakup regimes of a liquid jet', Ph.D. Thesis, Princeton Univ., 1978.

13) Hiroyasu, H. and Kadota, T., 'Fuel droplet size distribution in diesel combustion chamber', SAE 740715.

14) Kuniyoshi, H., Tanabe, H., Sato, T. and Fujimoto, H., 'Investigation on the characteristics of diesel fuel spray', SAE 800968.

15) Yule, A.J., Mo, S.L., Tham, S.Y. and Aval, S.M., 'Diesel Spray Structure', Proc. of the ICLASS-85 conference, paper 11B/2, 1985.

16) Elkotb, M.M., 'Fuel atomization for spray modelling', Prog. Energy Combust. Sci., 1982, Vol. 8, pp. 61-91.

17) Igura, S., Kadota, T. and Hiroyasu, H., 'Spontaneous ignition delay of fuel sprays in high pressure gaseous environments', Translated from JSME, Vol. 41, No. 345, pp. 1559 to 1566, 1975.